Exploitation of the far-offshore wind energy resource by fleets of energy ships - Part 2: Updated ship design and cost of energy estimate

Aurélien Babarit[1,2], Félix Gorintin[2,3], Pierrick de Belizal[3], Antoine Neau[3], Giovanni Bordogna[4], Jean-Christophe Gilloteaux[1]

[1]LHEEA, Ecole Centrale de Nantes - CNRS, Nantes, 44300, France
[2]INNOSEA, Nantes, 44300, France
[3]Farwind Energy, Nantes, 44300, France
[4]Blue Wasp Marine, Rotterdam, 3035TA, The Netherlands

Correspondence to: Aurélien Babarit (aurelien.babarit@ec-nantes.fr)

Abstract. This paper deals with a new concept for the conversion of far-offshore wind energy into sustainable fuel. It relies on autonomous sailing energy ships and manned support tankers. Energy ships are wind-propelled ships that generate electricity using water turbines attached underneath their hull. Since energy ships are not grid-connected, they include onboard power-to-X plants for storage of the produced energy. In the present work, the energy vector X is methanol.

In the first part of this study, an energy ship design has been proposed and its energy performance has been assessed. In this second part, the aim is to update based on design progression the energy and economic performance of such system.

In collaboration with ocean engineering, marine renewable energy and wind-assisted propulsion experts, the energy ship design of the first part has been revised. Based on this new design, a complete FARWIND energy system is proposed, and its costs (CAPEX and OPEX) are estimated. Results of the models show (i) that this FARWIND system could produce approximately 70,000 tonnes of methanol per annum (approximately 400 GWh per annum of chemical energy) at a cost in the range 1.2 to 3.6 €/kg, (ii) that this cost may be comparable to that of methanol produced by offshore wind farms in the long term, and (iii) that FARWIND-produced methanol (and offshore wind farms-produced methanol) could compete with gasoline on the EU transportation fuel market in the long term.

1 Introduction

To date, fuels such as oil, natural gas and coal account for approximately 80% of primary energy consumption globally (BP, 2018). Although this share is expected to decrease with the development of renewable power generation and the electrification of the global economy, some sectors may be difficult to electrify (e.g., aviation, freight). Therefore, if a global temperature change of less than 2°C—as set out in the Paris agreement—is to be achieved, there is a critical need to develop carbon-neutral alternatives to fossil fuels.

To address this challenge, we proposed in (Babarit et al., 2019) an energy system (FARWIND) which could convert the far-offshore wind energy resource into a sustainable fuel using fleets of energy ships, see Fig. 1. Energy ships are ships propelled by the wind which generate electricity by means of water turbines attached underneath their hulls. The generated electricity is converted into fuel using onboard power-to-gas (PtG) or power-to-liquid (PtL) plants. Hydrogen was not retained because it was found in Babarit et al. (2018) that hydrogen storage and transportation costs could account for nearly half of the cost of the delivered hydrogen when it is produced far-offshore (because of the low volumetric energy density at ambient temperature and pressure conditions which is a well-known challenge for hydrogen storage and transportation). In contrast, the other possible energy vector options (synthetic natural gas (SNG), methanol, or Fischer–Tropsch fuel (FT fuel), Graves et al., 2011; and ammonia, Morgan, 2013) are much simpler to store, transport and distribute (particularly methanol and FT fuel, as they are liquid for standard conditions of temperature and pressure). Moreover, they can be incorporated into existing infrastructure with little to no modification. The drawback is that they each require the supply of an additional feedstock (carbon dioxide or nitrogen depending on the energy vector) and an additional conversion step in the energy conversion process. The additional conversion step decreases the overall energy efficiency and increases the size and complexity of the PtX plant. In a previous study (Babarit et al., 2019), we investigated whether these drawbacks could be compensated for by the easier storage, transportation and distribution of the products, and we found that methanol is the most promising solution; hence it is retained as the energy vector in this study.
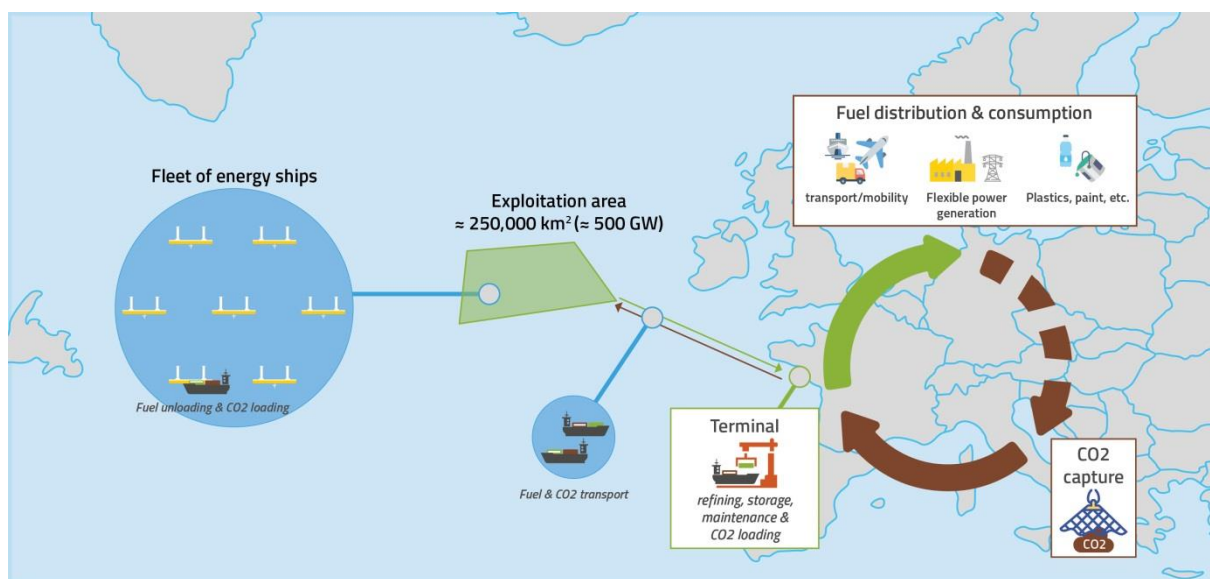
Figure 1 The concept of sustainable methanol production from far-offshore wind energy by FARWIND energy systems.

The produced methanol is collected by tankers which are also used to supply the energy ships with the necessary feedstock (carbon dioxide) for power-to-methanol conversion. Of course, the CO_2 supply source must be carbon-neutral for that system to produce sustainable methanol. Therefore, the CO_2 must be captured either directly or indirectly from the atmosphere.

Possible options include direct air capture (Keith et al., 2018), CO_2 capture from flue gases from biomass or FARWIND-produced methanol combustion, and CO2 from biogas upgrading (Li et al., 2017; Irlam, 2017).

The overall aim of the present study is to investigate the energy and economic performance of the FARWIND energy system. A preliminary energy ship design was proposed in (Babarit et al., 2020) and its energy performance was investigated. The cost of energy was estimated in (Babarit et al., 2020b). It was found that an initial FARWIND system could produce approximately 100,000 tonnes of methanol per at a cost in the range 0.9 to 2.1 €/kg.

This preliminary design has been reviewed by ocean engineering and marine renewable energy's experts of the Marine Energy Alliance European project (EMEC, 2020); and wind-assisted propulsion experts (Blue WASP, 2020). Based on their feedback, the ship design has progressed; and the economic model has been refined. The aim of the present paper is to present that improved design, the economic model, and the resulting levelized cost of energy. The present study also provides an example of how cost estimates develop throughout subsequent design stages.

The remainder of this paper is organized as follows. In section 2, the specifications of the updated design and its velocity and power performance are presented. In section 3, the specifications of the proposed energy system are presented, and its annual methanol production is estimated. Estimates of expenditures for the proposed energy system are provided and discussed in section 4. Using those estimates and the estimates of annual methanol production, the cost of energy is estimated in section 5 and market perspectives are discussed. Conclusions are presented in Section 6.

2 Specifications of the updated energy ship design
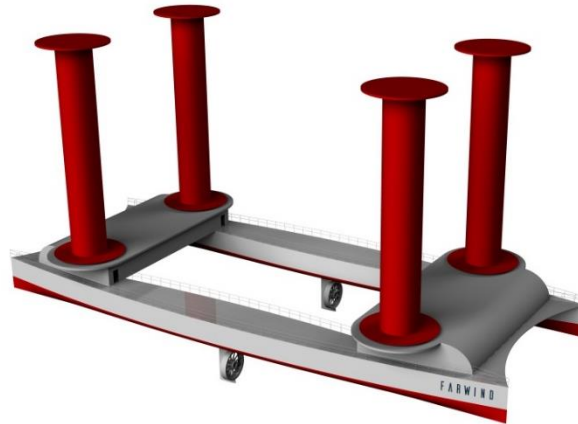
Figure 2 Artist's view of the proposed energy ship design.

The energy ship design considered in this study is a revision of that presented in (Babarit et al., 2020), see Fig. 2. It is still an 80 m long catamaran with four 5 m diameter Flettner rotors and two water turbines. The hull shape is the same. However, the height of the Flettner rotors is increased from 30 m to 35 m, and the rated power of each water turbine is reduced from 900 kW to 800 kW. The complete characteristics of the ship are summarized in Tab. 1. Explanations for the data shown in the table are provided in the following sections.

	Unit	Value
Hull		
Length	m	80
Breadth	m	31.7
Draught	m	2.1
Displacement	t	1,035
Structural mass	t	560
Wind propulsion		
Type	-	Flettner rotors
Number	-	4
Rotor height	m	35
Rotor diameter	m	5
Rotor mass	t	79
Rotor drive power (max)	kW	143
Water turbine		
Number	-	2
Turbine diameter	m	4
Rotor-to-electricity efficiency (η_3)	-	75%
Turbine mass	t	15
Rated power	kW	800
Auxiliaries subsystems		
Power consumption	kW	50
Auxiliaries subsystems mass	t	41
Power-to-methanol plant		
Electrolyzer rated power	kW	1,130
Electrolyzer mass	t	28
Desalination unit rated power	kW	Negligible
Desalination unit mass	t	Negligible
H_2tMeOH plant capacity	kg/h	100
H_2tMeOH plant mass	t	17
Storage tanks		
CO_2 storage capacity	t	23
CO_2 storage tank mass (empty)	t	15
Methanol storage capacity	t	17
Storage tank mass	t	4

Table 1 Specifications of the updated energy ship design

2.1 Rotors

The rotors technical specifications (dimensions, mass, maximum rotor drive power) used in this study are based on that of the largest currently available Flettner rotor (Norsepower, 2021).

80   The propulsive force (thrust) T of a Flettner rotor depends on the lift coefficient C_L, the drag coefficient C_D, the apparent wind speed V, the apparent wind angle α, the rotor area A (height times diameter) and the air density ρ_a:

$$T = \frac{1}{2}\rho_a A V^2 (C_L \sin \alpha - C_D \cos \alpha)$$

(1)

The lift coefficient and the drag coefficient depend on the ratio of the rotational velocity of the rotor to the apparent wind
85 speed (spin ratio SR). In (Babarit et al., 2020), we used the experimental data of (Charrier, 1979) for the aerodynamic coefficients of a Flettner's rotor as function of the rotor's spin ratio SR. However, these experiments were carried out at low Reynolds numbers (~10,000), with the Reynolds number defined as:

$$Re = \frac{VD}{\nu}$$

(2)

90 where ν is the kinematic viscosity and D is the rotor diameter. Recently, formulas based on full scale data (Reynolds number over 10^6) have been published (Tillig & Ringsberg, 2020). That data has been used in the present study (Figure 3) as it corresponds better to real conditions.

Moreover, rotors must be powered for them to spin. In (Babarit et al., 2020), we assumed that the rotors power consumption is constant (four times 40 kW), whereas in practice it depends on the wind loading. In their work, (Tillig & Ringsberg, 2020)
95 have developed a formula to estimate a rotor's power consumption as function of the spin ratio. We used that formula in the present study.
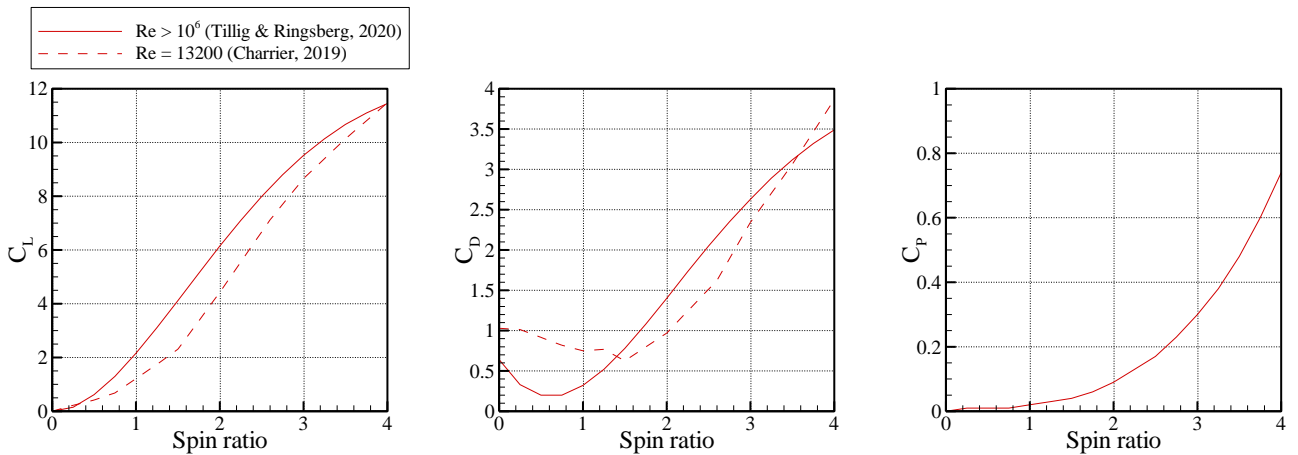
Figure 3 Comparison of aerodynamic coefficients of Flettner rotors according to (Charrier, 1979) and (Tillig & Ringsberg, 2020)

In (Babarit et al., 2020), the effect of aerodynamic interactions between rotors was neglected. In the present study, it has
100   been estimated using the approach proposed by (Roncin & Kobus, 2004) in which each rotor is modelled by a horseshoe
vortex. The implementation follows that of (Bordogna, 2020).

	Total	FR #1	FR #2	FR #3	FR #4
with interactions (kN)	353	117	99	86	51
without interactions (kN)	508	127	127	127	127
Interaction effect (kN)	69%	92%	78%	68%	40%
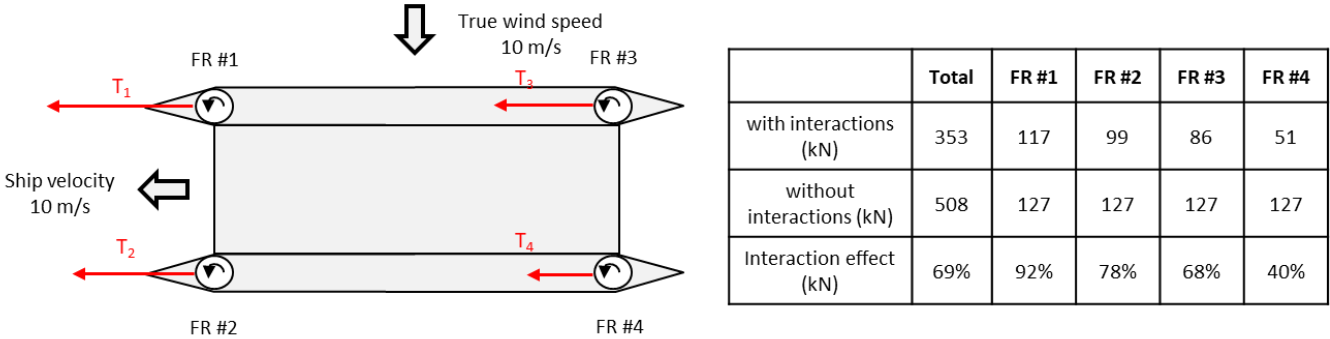
Figure 4 Effect of aerodynamic interactions on the propulsive force

105   The total propulsive force (with and without aerodynamic interactions) and the propulsive force from each rotor are shown in
Figure 4 for rated conditions (10 m/s true wind speed, 90° true wind direction, $SR = 3$, 10 m/s ship velocity). They show that
the interaction effect cannot be neglected as the total propulsive force is 69% of that without interactions. A similar
interaction effect has been found for other wind speeds (not reported here). Consequently, the model has been updated. The
total propulsive force (Eq. 1) has been reduced by a constant factor of 30% for all wind conditions.

110   The Earth atmospheric boundary layer was also not considered in the energy performance estimate in (Babarit et al., 2020).
In the present study, a power law has been assumed with an exponent of 0.14. Thus, in the updated model, the wind speed W
in Eq. 3 of (Babarit et al., 2020) is given by:

$$W = W_{10} \left(\frac{Z}{10}\right)^{0.14}$$

(1)

115   Where Z is 22.5 m (half the height of the rotor + 5 m).

2.2 Hull

The hull shape is the same as for the preliminary design. However, the hull mass estimate has been refined. The revised mass
estimate is based on a preliminary scantling of the hull structure which has been developed using rule NR600 of Bureau
Veritas (EMEC, 2020). The corresponding hull weight estimate is 560 t, which is more than twice the estimate of the
120   preliminary design. Moreover, the updated design assumes taller rotors (35 m), which are 20 tons heavier than the 30 m
rotors of the preliminary design. Consequently, the total displacement of the updated design is 1,035 tons (660 tons for the
preliminary design). The draught has increased from 1.6 m for the initial design to 2.1 m for the updated design.

Due to the increased displacement, the wetted surface increases to 1,064m². The wave resistance coefficient has also been updated (see Figure 5). As for the preliminary design, it was calculated using the software REVA (Delhommeau and Maisonneuve, 1987). One can see that the residuary resistance coefficient (wave making) is greater for the updated design than for the initial design, which is due to the increased displacement.
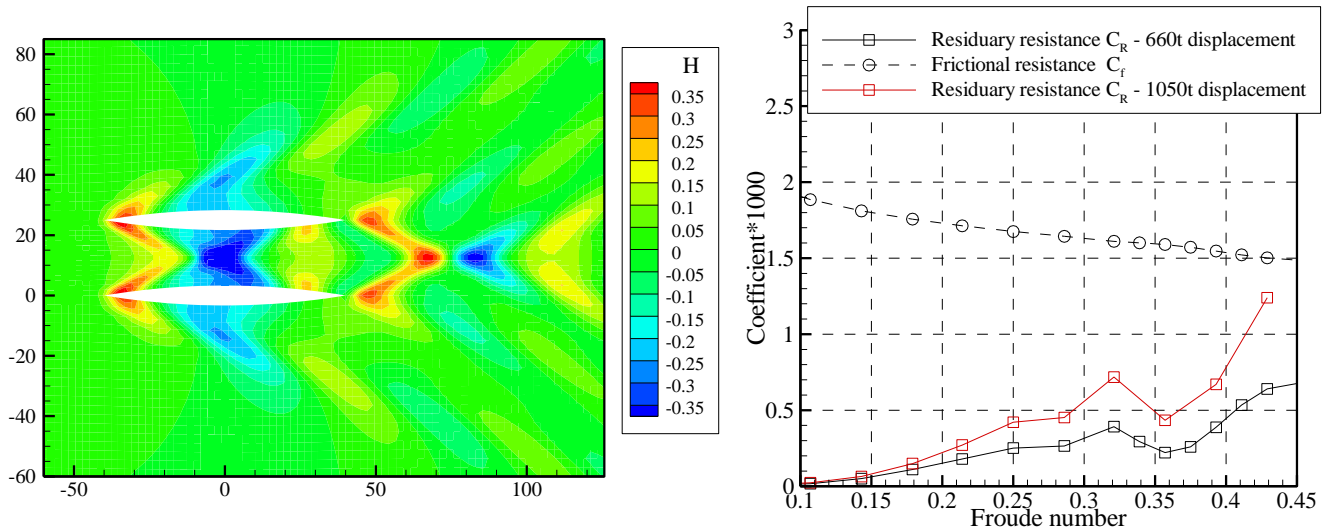
Figure 5 Left: wave pattern around the ship hull of the updated design for Froude number = 0.357 (10 m/s ship velocity). Right: hydrodynamic coefficients of the initial and updated design.

2.3 Water turbine

The water turbines' dimensions are the same as for the initial design (4 m diameter rotor). However, their mass is increased to 15 tons each (7.4 tons each for the initial design). Based on expert's advice, the water turbine's energy efficiency has been reduced to 75% (80% for the initial design). The rated power is decreased to 800 kW (900 kW for the initial design).

2.4 Power-to-methanol plant

For rated wind conditions (10 m/s true wind speed, 90° true wind angle), the ship velocity is almost 10 m/s (see section 2.7). The water turbines' power production is 1,600 kW. The Flettner rotors' power consumption is approximately 420 kW. Assuming a further 50 kW power consumption for the auxiliary subsystems, the net power production available to the electrolyzer of the power-to-methanol plant is 1,130 kW (1,420 kW for the initial design). The weight estimate of an electrolyzer of such rated power is 28 t (35 t for the initial design).

Assuming the same 60% efficiency for the electrolyzer and the same 78% efficiency for the hydrogen-to-methanol plant as for the initial design (Babarit et al., 2020), the rated power of the hydrogen-to-methanol plant is 680 kW (850 kW for the initial design). Its weight estimate is 17 t (24 t for the initial design).

2.5 Storage tanks

The capacities of the storage tanks (CO_2 and methanol) are set such as they can accommodate 7 days of production at rated
145   power (approx. 17 t of methanol). Thus, the CO_2 tank weight is 15 t and that of the methanol tank is 4 t (Babarit et al., 2020).

2.6 Auxiliary equipment

As for the initial design (Babarit et al., 2020), the weight of the auxiliary subsystems is taken equal to 10% of the total mass
budget excluding the hull weight (41 t).

2.7 Power production charts
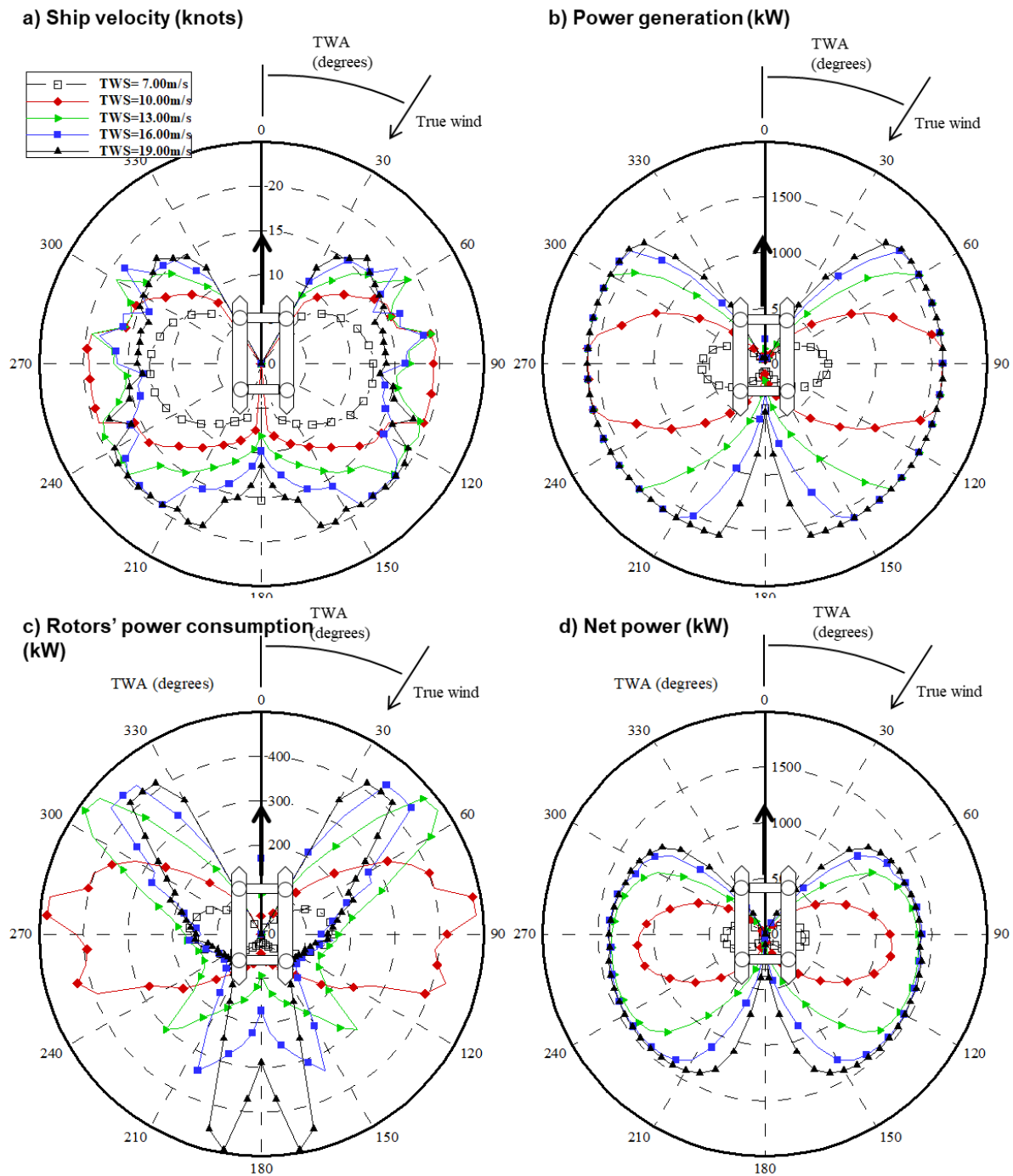
Figure 6 Ship velocity (a), power generation (b), rotors power consumption (c) and net power (d) of the updated ship design as function of wind conditions. TWA stands for true wind angle.

150

The velocity and power performance of the updated design has been calculated using the model presented in (Babarit et al., 2020). The results are shown in Figure 6 as function of the wind conditions (true wind speed and true wind angle).Note that for each data point, the water turbine's induction factor and the rotors' spin ratio were optimized in order to maximize power production while satisfying the constraints (maximum rotation velocity and thrust force for the rotors, maximum power generation for the water turbine).

Overall, the velocity and power performance of the updated design resemble that of the initial design (albeit 10 to 20% smaller). As for the initial design, rated power (1,600 kW) is achieved from a true wind speed of 10 m/s and a true wind angle of 90°. However, a major difference is that the rotors power consumption depends on the spin ratio in the updated design velocity and power performance prediction model, whereas it was fixed in (Babarit et al., 2020). Therefore, the net power keeps increasing with increasing wind speed (see panel (d)) despite the generated power has reached rated power (1,600 kW).

As for the initial design, the water turbine's induction factor and the rotors' spin ratio were optimized to maximize power production for each data point while satisfying constraints (maximum rotation velocity and thrust force for the rotors, maximum power generation for the water turbine). Due to those constraints, there can be several settings (induction factor, spin ratio) for the same power generation, which explain the noisy behavior for the ship velocity in panel (a).

3 Specifications of the proposed FARWIND energy system

In the FARWIND energy system concept, the energy ships are deployed in fleets and are supported by tankers which collect the produced methanol and transport it to a shore-based terminal, see Figure 1. The tankers also provide the energy ships with CO_2. In this section, we estimate the characteristics and number of the tankers, and the number of energy ships in a FARWIND system.

3.1 Tanker design

In the considered energy ship design, the methanol storage tank capacity allows storage of one week of methanol production at full capacity. Therefore, each energy ship of the fleet must meet a tanker for methanol collection and CO_2 refill at least once a week (to avoid stops in the production process because the methanol tank is full or because the CO_2 tank is empty).

Thus, let us estimate the number of energy ships that can be served by one tanker. This depends on the duration of the CO_2-loading and methanol-unloading operations. We assume that these operations take six hours on average, and that they are carried out continuously (including at night). Therefore, one tanker can service 28 energy ships per week (7 days/week x 24 hours/day / 6 hours/operation). As the capacity of an energy ship's methanol tank is 17 tonnes (23 tonnes for the CO_2 tank), the tanker may collect up to 473 t of methanol and supply 650 t of CO_2 every week.

It is assumed that the tankers are operated by a crew, and that the duration of their mission is four weeks. At the end of each four-weeks mission, the tanker returns to a shore-based terminal to change crew, unload the methanol, and load CO_2.

185 Therefore, their total methanol capacity must be 1,891 t (4 weeks x 473 t/week) and their total CO_2 capacity must be 2,601 t (4 w x 650 t/w). Assuming the CO_2 will be stored as liquid in a cryogenic storage tank, and extrapolating from (Chart, 2019), the empty weight of a 2,600 t capacity CO_2 storage vessel is estimated to be 1,700 t. For methanol, the mass of the required tank is estimated to be 410 t. The tanker will be carrying maximum cargo weight (4,720 t) when it leaves the terminal (full CO_2 tank and empty methanol tank). This cargo weight is relatively similar to the average vessel size of small crude oil

190 (3,600 deadweight (dwt)), chemical (4,900 dwt) and LPG vessels (3,500 dwt) (Lindstad et al., 2012). According to (MAN Energy Solutions, 2019), the propulsion power of a 5,000 t deadweight bulk carrier is 1,410 kW for a service speed of 12 knots. These are the values which we used for the service speed and propulsion power of the tanker.

3.2 FARWIND system design

Following (Babarit et al., 2018), it is assumed that the fleet of energy ships is deployed at a distance of 1,000 km from the

195 terminal. Therefore, the tankers must travel 1,000 km to meet the energy ships, and a further 1,000 km when returning to the terminal. At a service speed of 12 knots, the tanker's round-trip will take 90 hours. Considering the duration of unloading/loading operations and other maintenance operations, we estimate that the tanker will be away from the fleet of energy ships for a duration of one week.

To ensure continuous operation of the energy ships, the tanker must be replaced immediately when it leaves the production

200 zone. Therefore, each group of 28 energy ships must be supported by more than one tanker. It can be shown that the minimum number of tankers per fleet must be at least 1.25, meaning that the optimal FARWIND system comprises a fleet of 112 energy ships supported by five tankers. Over a year, the number of roundtrips between the terminal and the production zone is 10.4 for each tanker. The maximum methanol production of that system (assuming 100% capacity factor for the energy ships) is approximately 100,000 t per annum.

205 ## 3.3 Annual methanol production of the proposed FARWIND system design

Since energy ships are mobile, their route schedules can be dynamically optimized based on weather forecasts in order to maximize energy production. This was performed using a modified version of the weather-routing software QTVLM (Abd-Jamil et al., 2019). The coordinates of the starting and arrival point are: N 50.5; W 18.9 (approximately 1,000 km from the port of Brest, France). Over the three years 2015, 2016 and 2017, it was found that an average capacity factor of over 75%

210 can be achieved.

That estimate does not consider downtime due to maintenance (availability). According to (Sheng, 2013) and (Pfaffel, 2017), the failure rate of wind turbines is in the order of one failure per annum. Given the greater complexity of the energy ship system (additional energy conversion subsystems in comparison to a wind turbine e.g. power-to-methanol plant), it is

assumed that the average failure rate of energy ships is two failures per annum. The corresponding downtime is driven by accessibility and repair time. As accessibility at sea can be challenging and as energy ships are mobile, it is assumed that most of the repairs are performed at a port. Moreover, it is assumed that despite the failure, the energy ship is able to sail to that port at an average velocity of 10 knots (corresponding to half the rated velocity) without assistance (e.g. tug boat). Assuming that the distance between the production area and a port (with a dedicated shipyard) is 1,000 kms, it would take approximately two days for that energy ship to go to the port. Assuming a further 3 days for the repair and 2 days for the energy ship to go back to the production area, the downtime per failure is 7 days. Thus, for a failure rate of two failures per annum, the total downtime per annum is two weeks corresponding to a 96% availability.

Taking into account that availability estimate, it appears that a capacity factor of 72% can be achieved. The corresponding annual methanol production would be 70,600 t per annum. Note that it would require the supply of 97,400 t of CO_2, as the production of 1 kg of methanol requires 1.38 kg of CO2.

For sake of illustration, let us estimate the number of 5,000 t bulk carriers which could be powered by a FARWIND system. As mentioned in section 3.1, their propulsion power is 1,410 kW for a service speed of 12 knts. Assuming that they would sail at that speed 292 days per year (80% of the time) and that their engine efficiency is 40%, the required chemical energy is approximately 24,700 MWh per year. 70,600 t of methanol corresponding to approximately 386,000 MWh of chemical energy, the designed FARWIND energy system could power approximately sixteen 5,000 t cargo vessels.

4 Estimation of expenditures

4.1 Capital cost of a first of a kind energy ship

	Cost (k€)
Energy ship	
Hull	1,100 – 2,200 k€
Flettner rotors	4,200 – 4,900 k€
Water turbines	1,300 – 2,700 k€
Auxiliaries, assembly and systems integration	1,300 – 2,000 k€
Electrolyzer	1,100 – 2,200 k€
H_2-to-methanol plant	400 – 700 k€
Fresh water production unit	Negligible
Liquid CO_2 tank	Negligible
Methanol tank	Negligible
Power-to-methanol plant indirect cost (installation and assembly, etc.)	300 – 2,900 k€

Total	9,300 – 16,700 k€

Table 2 Estimates of the capital cost of a prototype of the proposed energy ship

Tab. 2 shows estimates of the capital cost of a prototype of the proposed energy ship.

The hull cost estimate was obtained using the usual approach which is to multiply the hull weight by a price per ton of fabricated steel. That price includes procurement and workforce required for hull construction. Thus, it depends on steel market price and shipyard location. The typical cost range is 2,000 €/t (South-East Asia construction) to 4,000 €/t (Northern Europe). The hull weight estimate being 560 t, we retain a hull cost in the range 1,100 to 2,200 k€.

According to (Kuuskoski, 2019), the cost of four 30 m Flettner rotors is in the range 3,000 to 3,500 k€. For four 45 m tall Flettner rotors, we assumed that the cost is approximately proportional to the rotor mass excluding foundation. That mass being 42 tonnes for a 30 m tall rotor and 59 tonnes for a 35 m tall rotor (Norsepower, 2021), we retain a Flettner rotors' cost in the range 4,200 to 4,900 k€.

The water turbine cost estimate assumes that it is proportional to its rated power. We assume that the price is in the range 800 to 1,700 €/kW, which yields a water turbine cost in the range 1,280 to 1,720 k€.

Ship common systems, ship assembly and systems integration typically represent 20% of the total cost of a ship according to (Shetelig, 2013). We applied this ratio to the sum of the hull cost, Flettner rotor cost and water turbines cost. The other equipments were not taken into account because their installation factor is taken into account separately.

Holl et al. (Holl et al., 2016) has developed scaling laws for the cost of the electrolyzer and the freshwater production unit based on market surveys. They depend on the nominal power of the equipment. Applying the electrolyzer scaling law to the 1,130 kW capacity electrolyzer of the energy ship results in an estimated cost of 1,400 k€, equivalent to 1,250 €/kW. This is in agreement with the range 1,000 to 1,950 €/kW reported in (Schmidt et al., 2017) for PEM electrolyzers (which we used in this study). As for the freshwater production, the application of the scaling law of Holl et al. yielded a cost estimate of 9 k€, which is very small in comparison to the other costs.

According to (Brynolf et al., 2018), the cost of a hydrogen-to-methanol plant is in the range 600 – 1,200 €/kW of methanol. As the estimated efficiency of the power-to-methanol conversion process is 49% (Babarit et al., 2020), it corresponds to 300 to 600 €/kW of electrolyzer input power. Thus, we retain 400 – 700 k€ for the hydrogen-to-methanol plant capital cost.

For the liquid CO_2 and methanol storage tanks, suppliers and prices can be found on the internet (e.g.(Gitank, 2021), (Chart, 2019)); typical costs are 300 €/ton of capacity for methanol and 1,000 €/ton of capacity for liquid CO_2. Overall, their costs are negligible in comparison to other costs.

The electrolyzer and hydrogen-to-methanol costs do not include installation and assembly, transportation, building, etc. Those costs are usually taken into account using an installation factor. According to (NREL, 2014), the lower end of the installation factor is 1.2 and up to 2 for the higher end. This leads to a cost of 300 – 2,900 k€.

4.2 Capital cost of a first of a kind FARWIND energy system

According to the discussion in section 3.2, a FARWIND energy system should include a fleet of 112 energy ships and 5 tankers. One can expect the unit cost for a fleet of 112 energy ships to be significantly smaller than the cost of an energy ship prototype. To take this into account, a learning rate of 10% was assumed on the unit cost of the energy ship as function of the built capacity, see Tab. 2. It can be noted that such learning rate corresponds to what was observed for wind turbines (Lindman and Soderholm, 2012). It leads to a range of capital cost of 620 to 1,110 M€ for the first fleet of energy ships. It corresponds to an average unit cost of 5,500 to 9,900 k€ per energy ship.

For the tanker, according to (Lindstad et al., 2012), the price of commercial ships is in the range 500 € to 4,750 € per ton of dwt, depending on the type of ships and size. The lower price is for crude oil tankers greater than 140,000 dwt, while the higher price is for roll-in/roll-off (ro-ro) ships of 7,000 dwt. In the present study, we retain a cost range of 2,500 to 4,000 €/ton of deadweight, leading to a tanker cost in the range 12,500 to 20,000 k€.

Thus, overall, the total capital cost of a FARWIND system comprised of 112 energy ships and 5 tankers is expected to be in the range of 680 to 1,210 M€ (3,700 to 6,700 k€ per megawatt of installed capacity).

4.3 Operational expenditures

Expected operation and maintenance (O&M) costs, including the cost of CO_2 supply, are summarized in Tab. 3 and detailed below.

	O&M cost (in % of capital cost of equipment per year)
Energy ship	
Hull	2%
Flettner rotors	3.5%
Water turbine	4 - 13%
Auxiliaries	2%
Electrolyzer	7.5 – 11.5%
H_2-to-methanol plant	9 - 13%
Fresh water production unit	10 - 20%
Liquid CO_2 tank	2%
Methanol tank	2%
Total	**4.8 – 8.5%**
Tanker	4 - 10%
FARWIND system	
Energy ships maintenance	24 – 58 M€/y
Tankers O&M	3 – 10 M€/y
CO_2 supply	2 – 19 M€/y

Insurance cost	4 – 15 M€/y
Total (including CO₂ supply and insurance cost)	**4.5 – 8.3%**

Table 3 Estimates of the operation and maintenance of a first-of-a-kind FARWIND energy system

4.3.1 Energy ships and tankers operation and maintenance cost

280 According to (Holl et al., 2016), the maintenance cost of the water turbine is in the range 4 to 13% of the capital cost, and that of the freshwater production unit is between 10 and 20%. According to (Chardonnet et al., 2017), the maintenance cost for the electrolyzer is in the order of 4% of capital cost. It is 2 -5% according to (Brynolf et al., 2018). It is unclear whether those maintenance takes into stack replacement. Indeed, PEM electrolyzers' stack lifetime is in the order of 50,000 hours. Thus, assuming a capacity factor of 72%, they would have to be replaced every 8 years. According to (Brynholf et al., 2018),

285 stack replacement cost is 60% of the electrolyzer cost. It leads to an additional 7.5% maintenance cost for the electrolyzer. Thus, we retain 7.5 – 11.5% for the maintenance cost of the electrolyzer. The same range is assumed for the hydrogen to methanol plant.

For the Flettner rotors, the maintenance cost is expected to be in the order of 3.5% of the rotors' capital cost (Kuuskoksi, 2020). For the other subsystems (hull, auxiliaries, storage tanks), it is expected that the maintenance costs would be small; a

290 2% maintenance cost was arbitrarily selected. Overall maintenance costs for the energy ship are thus in the order of 3.7 to 5.3%.

For the tanker, following (Holl et al., 2016), we estimate operation and maintenance costs to be 4 to 10%.

4.3.2 CO₂ supply cost

The ambition of the FARWIND energy system is to provide a sustainable alternative to the use of liquid fossil fuels (e.g.

295 oil). Therefore, as mentioned in the introduction, the CO_2 must be captured directly or indirectly from the atmosphere.

According to (Keith et al., 2018), the cost for direct air capture (DAC) using large-scale wet absorption DAC technology is in the range 80 to 204 €/ton of CO_2. The cost of CO_2 capture from biogas upgrading is in the order of 15 to 100 €/ton of CO_2 (Li et al., 2017). In the case of CO_2 capture from flue gases from combustion of biomass or FARWIND-produced methanol, the cost of carbon capture is in the order of 35 to 50 €/ton (assuming that it would be similar to that for capture of CO_2 from

300 power production processes involving coal or natural gas (Irlam, 2017)). Note that for both biogas upgrading and biomass or methanol combustion, the CO_2 concentration in the source is much greater than in ambient air, which results in a more effective capture than with DAC.

Carbon dioxide may also be extracted from seawater (Willauer et al., 2012). Indeed, some of the CO_2 present in the atmosphere dissolves in the ocean. However, this new technology is in its early stages of development (Willauer et al.,

305 2017).

In any case, the captured CO_2 must be liquefied for efficient transportation. The energy requirement for CO_2 liquefaction is in the order of 0.1 kWh/kg$_{CO2}$ according to (Oi et al., 2016), which is low; hence its associated cost is expected to be negligible.

Therefore, we estimate the cost of CO_2 production to be in the range 20 to 200 €/ton. As 97,400 t of CO_2 are required to produce 70,600 t of methanol, the CO_2 supply cost is estimated to be in the range 2–20 M€ per annum.

4.3.3 Insurance cost

Insurance cost is generally taken as 0.6% of CAPEX per year for vessels at the concept stage. However, for a new technology, this percentage of CAPEX may be higher, potentially as high as 1 - 2%. In this study, we have retained 0.6 – 1.2%.

4 Cost of energy estimates

4.1 Short-term cost

The levelized cost of methanol *LCOM* can be calculated as (Holl et al., 2016):

$$LCOM = \frac{CRF + \lambda}{AMP} I$$

(3)

where I is the total capital cost, λ is the total O&M rate, AMP is the annual methanol production, and $CRF = \frac{i(1+i)^n}{((1+i)^n - 1)}$ is the capital recovery factor, in which i is the weighted average cost of capital (WACC) and n is the lifetime in years. Assuming a WACC in the range 6–10% and a lifetime of 20 - 25 years, the capital recovery factor is in the range 7.8–11.7%. The methanol cost is thus in the range 1.2–3.6 €/kg (225 to 660 €/MWh$_{th}$). Note that the low end of the range (respectively high end) was obtained by using the most optimistic cost data (respectively most pessimistic cost data).

This cost is three to nine times greater than current market price for methanol (0.4 €/kg ≈ 72 €/MWh in the first quarter of 2021). However, it does not consider a price on GHG emissions. At least 0.675 kg of CO_2 is produced per kg of methanol produced using conventional processes (which are based on coal or natural gas) (Martin and Grossmann, 2017). In 2018, the carbon tax was 44.6 €/ton in France and 110 €/ton in Sweden; if CO_2 emissions were taken into account, the methanol price would increase by 6 €/MWh$_{th}$ and 13 €/MWh$_{th}$ respectively. Thus, unfortunately, even with a rather significant carbon tax, the cost of methanol produced with a first-of-a-kind FARWIND system would not be competitive.
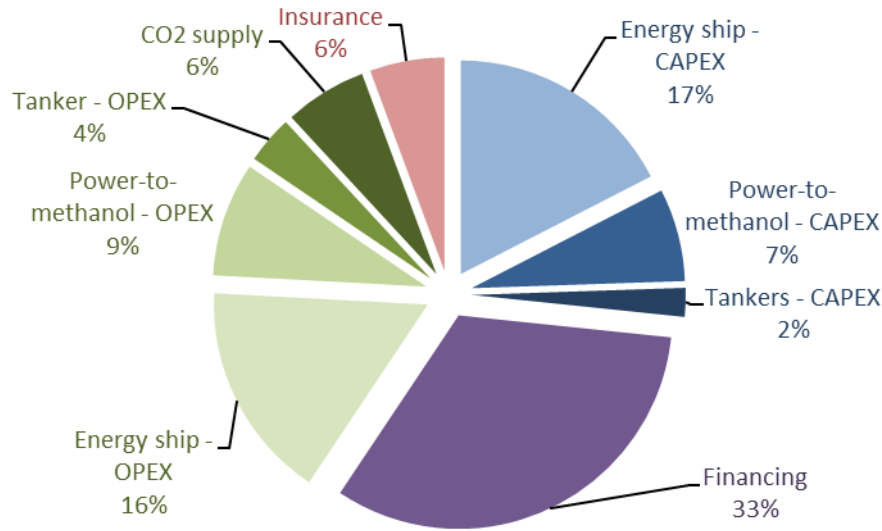
Figure 7 Cost breakdown of methanol produced by a first-of-a-kind FARWIND system. The shown data corresponds to an average cost scenario (methanol cost equal to 2.4 €/kg).

Figure 7 shows the cost breakdown for an average cost scenario. One can see that the main cost sources are the financing cost (33% of total methanol cost), the energy ship's capital cost (hull + Flettner rotors + water turbines + auxiliaries and integration, 17% of total methanol cost), and operation and maintenance cost of the FARWINDERs (16%). The total cost of energy storage - including the power-to-methanol plants capital cost and maintenance cost, CO2 supply, and tankers capital cost and operation and maintenance cost - accounts for 25% of total cost.

4.2 Comparison with methanol production by offshore wind turbines

Let us compare the cost of methanol production by FARWIND systems and offshore wind turbines. In this respect, we assume that the first-of-a-kind FARWIND system is deployed by 2030. At that time, according to (IRENA, 2019), the global offshore wind energy capacity will have reached 230 GW.

The key economic drivers in power-to-gas or power-to-liquid processes are the cost of input electricity to the power-to-gas/liquid plant and the power-to-gas/liquid plant capacity factor (Fasihi et al., 2016; Ioannou and Brennan, 2019). Based on that data, one can calculate the methanol production cost using:

$$LCOM = \frac{(CRF + \lambda')I'}{8760 \times C_F \times P_{rated} \times \eta_{MeOH}} + \frac{LCOE_{elec}}{\eta_{MeOH}} + 1.38 \times \frac{C_{CO2}}{LHV_{MeOH}}$$

(4)

where I' is the capital cost of the power-to-methanol plant, λ' is the O&M rate of the power-to-methanol plant plus the insurance rate, C_F is the plant capacity factor, P_{rated} is the rated power of the plant, η_{MeOH} is the plant efficiency (49%, see (Babarit et al., 2020)), $LCOE_{elec}$ is cost of input electricity to the power-to-methanol plant, C_{CO2} is the CO_2 cost per unit mass and LHV_{MeOH} is the lower-heating-value of methanol per unit mass (the factor 1.38 corresponds to the fact that it takes 1.38 kg of CO_2 to produce 1 kg of methanol).

CAPEX	480 – 1,285 €/kW
OPEX	6 – 7%
CO_2 supply cost	20 – 200 €/t
Insurance	0.6 – 1.2%
Lifetime	20 – 25 y
WACC	6 – 10%

Table 4 Expected costs of a power-to-methanol plant by 2030 (excluding input electricity)

Table 4 shows the cost assumption for the power-to-methanol plant of the offshore wind farm. The capital cost is assumed to be a third of that of the first-of-a-kind FARWIND system as the power-to-methanol plant would be much larger (Brynolf et al. 2018) and as it may be shore-based. According to (IRENA, 2019), the cost of electricity from offshore wind farms will be in the range 40 to 80 €/MWh by 2030 with capacity factors in the range 36 to 58%. Therefore, using Eq. 4, we find that the methanol production cost by offshore wind farms would be in the range 110 to 375 €/MWh$_{th}$ (0.6 to 2.1 €/kg) by 2030. Thus, by 2030, the cost of methanol produced by a FARWIND energy system (1.3 to 2.1 €/kg) would not be competitive with that produced by a shore-based power-to-methanol plant powered by a large offshore wind farm.

However, that would be the case for a first of a kind for FARWIND, whereas it would be for an expected global capacity of 230 GW for offshore wind turbines. Therefore, provided that sufficient FARWIND capacity is installed, FARWIND-produced methanol may become comparable to that of offshore wind farms-produced methanol. This is shown in Figure 8 which shows a comparison of the long-term methanol cost produced by FARWIND systems and by offshore wind farms. A learning rate of 10% was assumed both for the FARWIND systems and for the methanol-producing offshore wind farms. However, for the offshore wind farm, it has been taken into account that the cost of input electricity assumes an installed 230 GW global offshore wind capacity. Therefore, it can be expected that it would take a further 230 GW to achieve a cost reduction of 10% of that part of the methanol cost (second term in Eq. 4.). Thus, the methanol production cost of offshore wind farms as function of the installed capacity C_{OW} (in GW) can be written:

$$LCOM_{OW}(C_{OW}) = \left(\frac{(CRF + \lambda')I'}{8760 \times C_F \times P_{rated} \times \eta_{MeOH}} + 1.38 \times \frac{C_{CO2}}{LHV_{MeOH}} \right) \times 0.9^{\log_2 \frac{C_{OW}}{0.2}} + \frac{LCOE_{elec}}{\eta_{MeOH}} \times 0.9^{\log_2 \frac{230+C_{OW}}{230}}$$

(5)

Note that, in agreement with the cost data of (Brynolf et al., 2018), it has been assumed that the capacity of the first methanol-producing offshore wind farm is 200 MW.
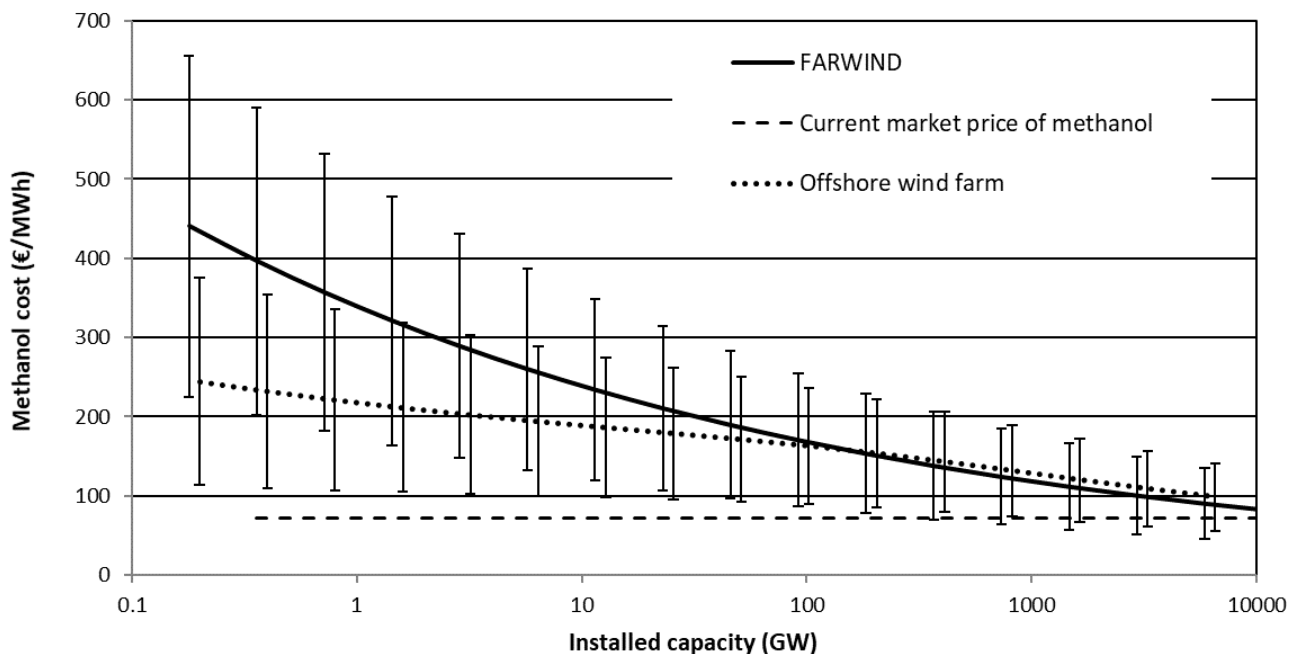
Figure 8 Comparison of long term methanol cost produced by FARWIND systems and offshore wind farms as function of the installed capacity

4.3 Long-term cost and market potential

Let us now consider the perspective of carbon-neutral methanol produced by FARWIND systems or offshore wind farms for the transportation fuel market. Indeed, methanol can be blended with gasoline in low quantities for use in existing road vehicles. According to (Methanol Institute, 2014), the blend can include up to 15% methanol by volume (M15 fuel). Moreover, flexible fuel vehicles which can run on an 85%–15% methanol–gasoline mix (M85 fuel) have been developed and commercialized (e.g. the 1996 Ford Taurus); and M100 (100% methanol) vehicles are in development (Olah et al., 2018). Thus, carbon-neutral methanol could be used as a low-carbon substitute to oil on the transportation fuel market.

390
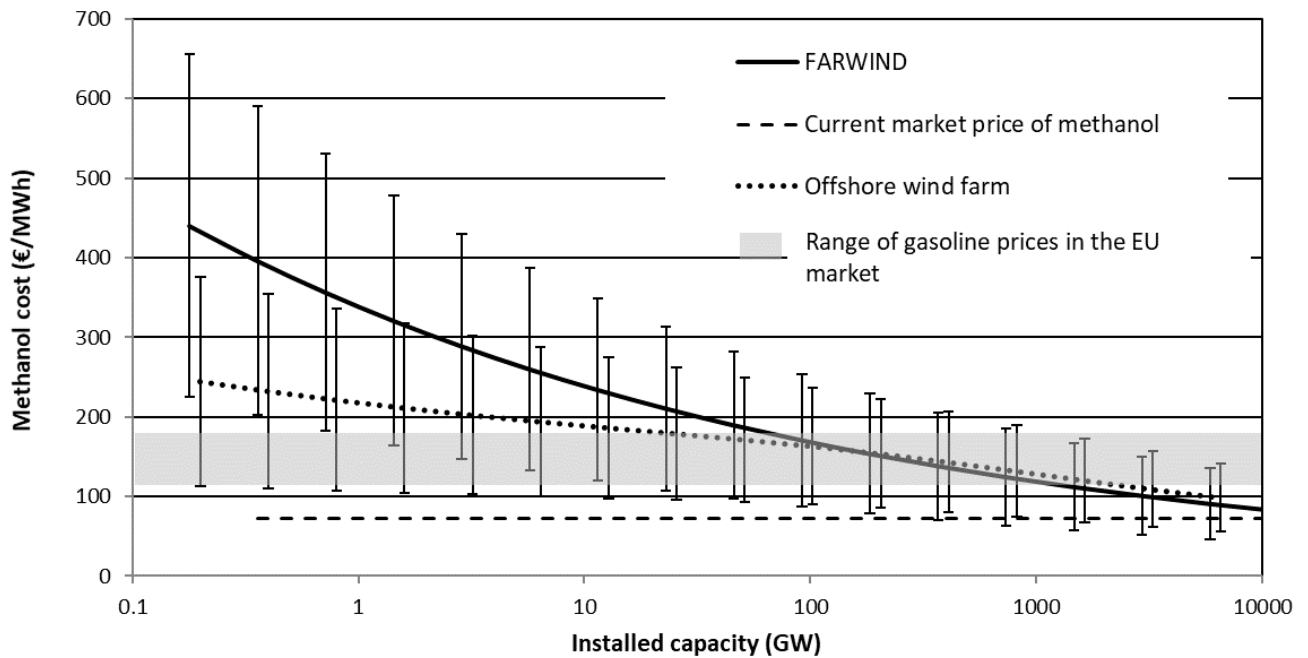
Figure 9 Cost of methanol produced by FARWIND systems and offshore wind farms as function of the installed capacity and comparison with current market price of gasoline in the EU

Let us compare the cost of FARWIND-produced and offshore wind farm-produced methanol to the gasoline price in the EU. Gasoline price ranges from 1.1 €/L (Bulgaria) to 1.7 €/L (Netherlands), the price differences arising from different
395 policies on fuel taxes in different countries (European Commission, 2019). This price range is equivalent to 112 to 173 €/MWh$_{th}$, since the standard density of gasoline traded in the EU is 0.755 kg/L and its energy content is approximately 13 kWh$_{th}$/kg. Thus, as can be seen in Figure 9 and provided that taxes policies are favourable, carbon-neutral methanol produced by offshore wind farms may already be competitive with gasoline on the EU transportation fuel market. For FARWIND-produced methanol, it may take "only" a few tens of GW of installed capacity to be competitive.

400 **4.4 Uncertainty discussion of cost of energy**

In the present study, the economic feasibility is based on broad assumptions that undoubtably include considerable uncertainty. That uncertainty has been taken into account by considering ranges for the cost parameters. The ranges were determined based on suppliers and/or experts' recommendations, and/or publicly available literature. The uncertainty was propagated by applying the most optimistic cost data (respectively most pessimistic cost data) to determine the low end
405 (respectively high end) of the levelized cost of methanol.

Regarding energy production, no uncertainty was applied. This is because energy production results from a deterministic numerical model. Comparisons with experiments (which are not yet available) are necessary to determine its level of accuracy. This may lead to the higher end of the cost of methanol estimate actually be underestimated should the actual energy production be significantly smaller than that predicted by the numerical model. On the other hand, if the design of the energy ship was optimized for the specific purpose of increased profitability, the proposed system might become significantly more competitive compared to the current design.

5 Conclusions

In this paper, we proposed an energy system for sustainable methanol production from the far-offshore wind energy resource. It is based on an autonomous fleet of 112 energy ships and 5 manned tankers for the collection and transport of the produced methanol, as well as the supply of CO_2 to the energy ships. Its methanol production is expected to be in the order of 70,600 t per annum (approximately 390 GWh per annum of chemical energy). The cost of this methanol is expected to be in the range 1.2–3.6 €/kg for the first-of-a-kind FARWIND system, which is significantly greater than the current market price for fossil fuel-derived methanol (0.4 €/kg). However, methanol can be used as a substitute to fossil fuels on the fuel transportation market: since the price of transportation fuel is high in most European countries, and assuming that a cost reduction similar to that observed for land-based wind energy can be achieved, the cost of FARWIND-produced methanol could compete with gasoline in the EU.

The cost of methanol produced by a first-of-a-kind FARWIND system is unlikely to be competitive with that produced by a large shore-based power-to-methanol plant powered by an offshore wind farm. However, provided that sufficient FARWIND capacity is installed, FARWIND-produced methanol may become comparable to that of offshore wind farms-produced methanol.

However, one should note that the present study is based on many broad assumptions that include considerable uncertainty. Further work is needed to confirm the findings. Moreover, one should note that the cost of FARWIND-produced methanol is based on a particular energy ship design, which might be optimized to reduce costs.

6 Code and data availability

The code and data supporting the findings of this study are available on request from the corresponding author.

7 Author contribution

Aurélien Babarit and Jean-Christophe Gilloteaux conceived of the presented idea. Aurélien Babarit developed the theory and performed the computations. Giovanni Bordogna contributed to the modelling of the aerodynamic interactions. Pierrick de Belizal, Antoine Neau and Félix Gorintin performed the structural analysis of the hull. Aurélien Babarit wrote the manuscript in consultation with all other co-authors.

8 Competing interests

Aurélien Babarit and Félix Gorintin are co-founders of Farwind Energy : www.farwind-energy.com, which aims at commercializing the technology described in the paper.

9 Acknowledgements

440 This research was partially carried out in the Marine Energy Alliance project, which is financially supported by Interreg North West Europe.

References

Abd-Jamil, R., Chaigneau, A., Gilloteaux, J-C., Lelong, P., Babarit, A.: Comparison of the capacity factor of stationary wind turbines and weather-routed energy ships in the far-offshore. In Journal of Physics: Conference series, 1356, 2019

445 BP: BP Statistical review of world energy, 67th edition, June 2018

Babarit, A., Gilloteaux, J-C., Clodic, G., Duchet, M., Simoneau, A., Platzer, M.F.: Techno-economic feasibility of fleets of far offshore hydrogen-producing wind energy converters. International Journal of Hydrogen Energy, 43(15), 7266-7289, 2018 https://doi.org/10.1016/j.ijhydene.2018.02.144

Babarit, A., Gilloteaux, J-C., Body, E., Hetet, J-F.: Energy and economic performance of the FARWIND energy system for

450 sustainable fuel production from the far-offshore wind energy resource. In Proc. Of the 14th International conference on ecological vehicles and renewable energies (EVER 2019), Monaco, 2019

Babarit, A., Clodic G., Delvoye S., Gilloteaux, J-C.: Exploitation of the far-offshore wind energy resource by fleets of energy ships. Part I. Energy ship design and performance. Wind Energy Science, 5, 839-853, 2020 https://doi.org/10.5194/wes-5-839-2020

455 Babarit, A., Delvoye, S., Clodic, G., and Gilloteaux, J.-C.: Exploitation of the far-offshore wind energy resource by fleets of energy ships. Part B. Cost of energy, Wind Energ. Sci. Discuss. [preprint], https://doi.org/10.5194/wes-2019-101, 2020.

Blue WASP: Preliminary analysis of Flettner rotor aerodynamic interaction for two given conditions, Technical report, 9 pp., November 2020

Brynolf, S., Taljegard, M., Grahn, M., Hansson, J.: Electrofuels for the transport sector: a review of production costs.

460 Renewable and sustainable energy reviews, 81, 1887-1905, 2018 https://doi.org/10.1016/j.rser.2017.05.288

Bureau Veritas: NR600 Hull structure and arrangement for the classification of cargo ships less than 65 m and non cargo ships less than 90 m, Edition Nov 2018. Available at https://marine-offshore.bureauveritas.com/nr600-hull-structure-and-arrangement-classification-cargo-ships-less-65-m-and-non-cargo-ships-less (last accessed 2021/2/19)

Chardonnet, C., De Vos, L., Genoese, F., Roig, G., Giordano, V., Rapoport, S., et al.: Study on early business cases for H2 in

465 energy storage and more broadly power to H2 applications. Tractebel & Hinicio. Final report, 2017

Charrier, D. : Etude théorique et expérimentale de l'effet "Magnus" destiné à la propulsion des navires. PhD thesis, Université de Paris VI, 1979

Chart, Technical manual: carbon dioxide storage tank. Manual #11650869 Rev, 2019

Delhommeau G., and Maisonneuve J-J.: Extensions du code de calcul de résistance de vagues REVA : prise en compte des effets de fond et de portance, Compte-rendu des 1ᵉ Journées de l'hydrodynamique, Nantes, France, 1987

EMEC: Marine Energy Alliance – FARWIND: feasibility review, Technical report, 24 pp., October 2020

European Commission: Consumer prices of petroleum products inclusive of duties and taxes. Prices in force on 18/11/2019, 2019

Fasihi, M., Bogdanov, D., Breyer, C.: Techno-economic assessment of power-to-liquids (PtL) fuels production and global trading based on hybrid PV-wind power plants, Energy procedia, 99, 243-268, 2016. https://doi.org/10.1016/j.egypro.2016.10.115

Holl, M., Rausch, L., Pelz, P.F.: New methods for new systems – how to find techno-economically optimal hydrogen conversion system. International Journal of Hydrogen Energy, 42, 22641-22654, 2017 https://doi.org/10.1016/j.ijhydene.2017.07.061

Gotz, M., Lefebvre, J., Mors, F., McDaniel Koch, A., Garf, F., Bajohr, S., Reimert, R., Kolb, T.: Renewable power-to-gas: a technological and economic review, Renewable Energy, 85, 1371-1390, 2016 https://doi.org/10.1016/j.renene.2015.07.066

Graves, C., Ebbesen, S. D., Mogensen, M., and Lackner, K. S.: Sustainable hydrocarbon fuels by recycling CO2 and H2O with renewable or nuclear energy, Renewable and Sustainable Energy Reviews, 15, 1–23, 2011. https://doi.org/10.1016/j.rser.2010.07.014

Ioannou, A., Brennan, F.: A techno-economic comparison between a grid-connected and non-grid connected offshore floating wind farm, In Proc. Of the IEEE 2019 Offshore energy and storage summit (OSES), Brest, France, 2019 https://doi.org/10.1109/OSES.2019.8867350

Keith, D.W., Holmes G., St Angelo, D., Heidel, K.: A process for capturing CO2 from the atmosphere, Joule, 2, 1573-1594, 2018. https://doi.org/10.1016/j.joule.2018.05.006

Gitank : https://www.gitank.com/methanol-storage-tanks (last accessed 2021/7/9)

IRENA: Future of wind – deployment, investment, technology, grid integration and socio-economic aspects. October 2010.

Irlam, L.: Global costs of carbon capture and storage – 2017 update. Global CCS institute, June 2017

Li, H., Tan, Y., Ditaranto, M., Yan, J., Yu, Z.: Capturing CO2 from biogas plants, Energy procedia, 114, 6030-6035, 2017. https://doi.org/10.1016/j.egypro.2017.03.1738

Lindman, A., Soderholm, P.: Wind power learning rates: a conceptual review and meta-analysis, Energy economics, 34, 754-761, 2012 https://doi.org/10.1016/j.eneco.2011.05.007

Lindstad, H., Asbjornslett, B.E., Stromman, A.H.: The importance of economies of scale for reductions in greenhouse gas emissions from shipping. Energy policy, 46, 386-398, 2012 https://doi.org/10.1016/j.enpol.2012.03.077

Kuuskoski, J.: Private communication, 2019

500   Kuuskoski, J.: Private communication, 2020

MAN Energy solutions: propulsion trends in bulk carriers, 2019

Martin, M., Grossmann, I.E.: Towards zero CO2 emissions in the production of methanol from switchgrass. CO2 to methanol. Computers and chemical engineering, 105, 308-316, 2017 https://doi.org/10.1016/j.compchemeng.2016.11.030

Methanol Institute, M15 methanol gasoline blends: 35 years of research and experience supports its use. Methanol facts,

505   2014

Moné, C., Stehly, T., Maples, B., Settle, E.: 2014 cost of wind energy review. Technical report NREL/TP-6A20-64281, National Renewable Energy Laboratory, Golden, CO, 2015

Morgan, E. R.: Techno-economic feasibility study of ammonia plants powered by offshore wind, Dissertations 697, University of Massachussets – Amherst, 2013.

510   Norsepower: Rotor   Sail   Technology.   Commercial   brochure,   2021.   Available   at https://www.norsepower.com/download/brochure.pdf (last accessed 2021/2/19)

Oi, L.E., Eldrup, N., Adhikari, U., Bentsen, M.H., Badalge, L., Yang, S.: Simulation and cost comparison of CO2 liquefaction, Energy procedia, 86, 500-510, 2016. https://doi.org/10.1016/j.egypro.2016.01.051

Olah, G.A., Goeppert, A., Surya Prakash, G.K.: Beyond Oil and Gas: the methanol economy. Third, updated and enlarged

515   edition. Wiley-VCH, 2018

Papanikolaou, A.: Chapter 2: Selection of main dimensions and calculation of basic ship design value. In: Ship Design: methodologies of preliminary design. Springer 628 pp., 2014

Pfaffel, S., Faulstich, S., Rohrig, K.: Performance and reliability of wind turbines: a review, Energies, 10, 2017 https://doi.org/10.3390/en10111904

520   Schmidt, O., Gambhir, A., Staffel, I., Hawkes, A., Nelson, J., Few, S.: Future cost and performance of water electrolysis: an expert   elicitation   study.   International   journal   of   hydrogen   energy,   42,   30470   –   30492,   2017 https://doi.org/10.1016/j.ijhydene.2017.10.045

Sheng, S.: Report on wind turbine subsystem reliability: a survey of various databases. Presentation NREL/PR-5000-59111, National Renewable Energy Laboratory, Golden, CO, June 2013

525   Shetelig, K.: Shipbuilding cost estimation: parametric approach. Norwegian University of Science and Technology, Trondheim, Norway. 61 pp, 2013

Tillig, F., Ringsberg, J.W.: Design, operation and analysis of wind-assisted cargo ships. Ocean engineering, 211, 107603, 2020 https://doi.org/10.1016/j.oceaneng.2020.107603

Willauer, H.D., Hardy, D.R., Schultz, K.R., Williams, F.W.: The feasibility and current estimated capital costs of producing

530   jet fuel at sea using carbon dioxide and hydrogen. Journal of Renewable and sustainable energy, 4, 2012 https://doi.org/10.1063/1.4719723

Willauer, H.D., DiMascio, F., Hardy, D.R.: Extraction of carbon dioxide and hydrogen from seawater by an electrolytic cation exchange module (E-CEM) part V: E-CEM effluent discharge composition as a function of electrode water composition. Washington D.C.: Naval research laboratory, 2017